

Condition monitoring methods, failure identification and analysis for Induction machines

Neelam Mehala, Ratna Dahiya

Abstract— Induction motors are a critical component of many industrial processes and are frequently integrated in commercially available equipment and industrial processes. The studies of induction motor behavior during abnormal conditions, and the possibility to diagnose different types of faults have been a challenging topic for many electrical machine researchers. The Motor Current Signature Analysis (MCSA) is considered the most popular fault detection method now a day because it can easily detect the common machine fault such as turn to turn short ckt, cracked /broken rotor bars, bearing deterioration etc. This paper presents theory and some experimental results of Motor current signature analysis. The MCSA uses the current spectrum of the machine for locating characteristic fault frequencies. The spectrum is obtained using a Fast Fourier Transformation (FFT) that is performed on the signal under analysis. The fault frequencies that occur in the motor current spectra are unique for different motor faults. However this method does not always achieve good results with non-constant load torque. Therefore, different signal processing methods, such as Short-time Fourier Transform (STFT) and Wavelet transforms techniques are also proposed and compared in this paper.

Keywords—Fault diagnosis, Fast Fourier transforms, MCSA, Short time Fourier transform (STFT), Wavelet transform

I. INTRODUCTION

ADVANCES in digital signal processing technology have enabled researchers to process more data in less time. As a result, information that is not previously available can be extracted from the collected data. In the light of these developments, condition monitoring via MCSA has recently drawn more attention from researchers. MCSA focuses its efforts on the spectral analysis of the stator current and has been successfully used in the detection of broken rotor bars, bearing damage and the dynamic eccentricity [1]. MCSA analyzes the stator current in search of current harmonics directly related to new rotating flux components, which are caused by faults in the motor-flux distribution [2]. The advantage of this technique is that it is well recognized nowadays as a standard due to its simplicity: It needs only one current sensor per machine and is based on straightforward

signal-processing techniques such as fast Fourier transforms (FFT). The MCSA uses the current spectrum of the machine for locating characteristic fault frequencies. The spectrum is obtained using a Fast Fourier Transformation (FFT) that is performed on the signal under analysis. But, the FFT in the stator current is quite difficult to apply with accuracy due to problems such as frequency resolution, magnitude accuracy at steady state, and more generally, due to data processing [3]. Therefore, this paper also discusses some new methods (Short Time Fourier Transform, Wavelet transform) based on stator-current analysis for online fault detection in induction machines, which would overcome the averaging problems of classical FFT.

Fourier analysis has some serious drawbacks. In transforming to the frequency domain, time information is lost. When looking at a Fourier transform of a signal, it is impossible to tell when a particular event took place. If the signal properties do not change much over time - that is, if it is what is called a stationary signal - this drawback isn't very important. However, most interesting signals contain numerous non-stationary or transitory characteristics: drift, trends, abrupt changes, and beginnings and ends of events. These characteristics are often the most important part of the signal, and Fourier analysis is not suited to detecting them. In an effort to correct this deficiency, Dennis Gabor (1946) adapted the Fourier transform to analyze only a small section of the signal at a time -- a technique called windowing the signal. Gabor's adaptation, called the Short-Time Fourier Transform (STFT), maps a signal into a two-dimensional function of time and frequency as shown in figure 1.

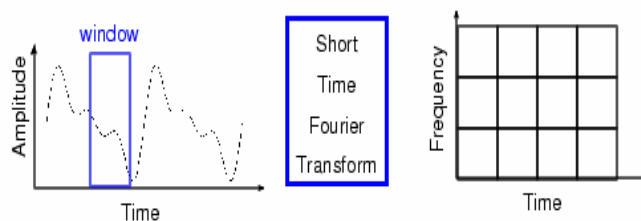


Figure 1: Short time Fourier transform

The STFT represents a sort of compromise between the time- and frequency-based views of a signal. It provides some information about both when and at what frequencies a signal event occurs. However, this information can be obtained with limited precision, and that precision is determined by the size of the window. While the STFT compromise between time and frequency information can be useful, the drawback is that once we choose a particular size for the time window, that

Manuscript received October 3, 2008; Revised version received February 23, 2009.

Neelam Mehala is with the Electronics and Communication Engineering Department, YMCA Institute of Engineering, Faridabad (Haryana) INDIA. (email address: neelamturk@yahoo.co.in)

Ratna Dahiya is with Electrical Engineering Department, National Institute of Technology, Kurukshetra, (Haryana) INDIA. (email address: ratna_dahiya@yahoo.co.in)

window is the same for all frequencies. Many signals require a more flexible approach -one where we can vary the window size to determine more accurately either time or frequency. For this, wavelet analysis can be used. Thus, Wavelet analysis represents the next logical step: a windowing technique with variable-sized regions. Wavelet analysis allows the use of long time intervals where more precise low-frequency information is required and shorter regions where high-frequency information is required.

The main aim of this paper is to discuss the importance of FFT, STFT and wavelet transforms methods for stator-current analysis to detect the faults in induction machines. Here, three different signal processing solutions are attempted: The first one is based on FFT, second is based on short-time Fourier transform (STFT) and third one on wavelet transform. The next section of this paper describes the most common faults in induction motors (IM) and their diagnosis using FFT. Novel approaches using STFT and wavelet decomposition are discussed in Section III and IV with some experimental results. Finally, Section V presents some concluding remarks.

II. FAULT DIAGNOSIS WITH FAST FOURIER TRANSFORMATION

MCSA depends upon locating by spectrum analysis specific harmonic components in the line current produced of unique rotating flux components caused by faults such as broken rotor bars, air-gap eccentricity and shorted turns in stator windings, etc. The motor current signature analysis method can detect these problems at an early stage and thus avoid secondary damage and complete failure of the motor. Note that only one current transducer is required for this method, and it can be in any one of the three phases [6]. The equipment setup for measuring motor current is shown in Figure 2.

motor, as shown in Figure 2(a). In the case of no secondary circuit, CT may be clamped onto one of the main phase leads to measure the motor phase current, as shown in Figure 2(b). The signal conditioning unit also provides proper high pass filtering for air-gap eccentricity test. It removes line frequency content since the amplitude of the line frequency is much greater than that of the eccentricity data [15]. It is very important to follow safety procedures at all times when motor current is measured. Another advantage of this method is that it can be also applied online. An idealized current spectrum is shown in Fig. 3.

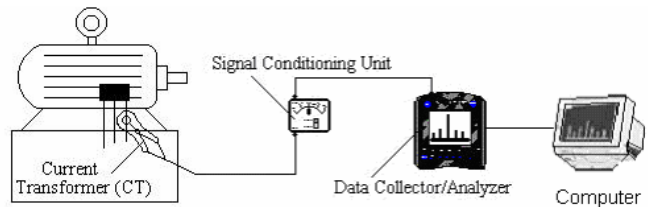


Figure 2(b): Main phase current measurement

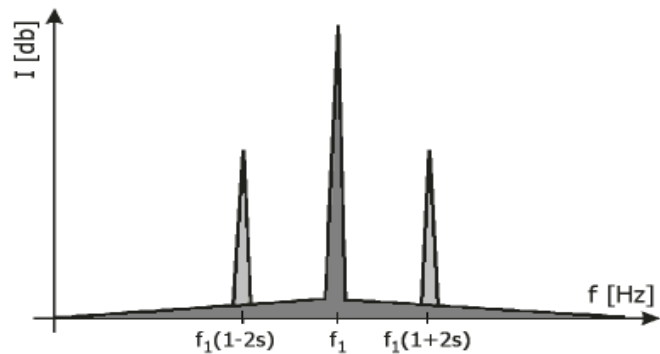


Figure 3 : Idealized current spectrum

The two slip frequency sidebands due to broken rotor bars near the main harmonic can be clearly observed. Usually a decibel (dB) versus frequency spectrum is used in order to give a wide dynamic range and to detect the unique current signature patterns that are characteristic of different faults [7, 8].

In the three-phase induction motor under perfectly balanced conditions (healthy motor) only a forward rotating magnetic field is produced, which rotates at synchronous speed, $n_1 = f_1 \cdot p$, where f_1 is the supply frequency and p the pole-pairs of the stator windings. The rotor of the induction motor always rotates at a speed (n) less than the synchronous speed. The slip, $s = (n_1 - n) / n_1$, is the measure of the slipping back of the rotor regarding to the rotating field. The slip speed ($n_2 = n_1 - n = s \cdot n_1$) is the actual difference in between the speed of the rotating magnetic field and the actual speed of the rotor.

The frequency of the rotor currents is called the slip frequency and is given by [9]:

$$f_2 = n_2 \cdot p = s \cdot n_1 \cdot p \quad \dots\dots(1)$$

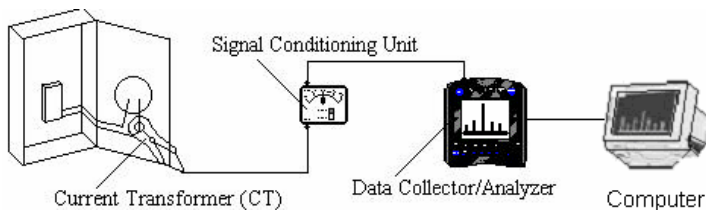


Figure 2(a): Secondary current measurement

Motor phase current is measured by a current transformer (CT). The signal is fed into a signal conditioning unit, which converts the measured current into voltage and also provides proper filtering. The output from the signal conditioning unit is connected to the data collection channel of a data collector/analyzer. There are two types of circuits for induction motors, namely main phase circuit and secondary circuit. The preferred method for motor current measurement is to clamp the CT onto the secondary circuit for the motor. This is a low amperage circuit, usually less than 5 amps, and is easily accessed in the switch gear cabinet for the induction

The speed of the rotating magnetic field produced by the current carrying rotor conductors with respect to the stationary stator winding is given by:

$$n + n_2 = n + n_1 - n = n_1 \quad \dots\dots(2)$$

With respect to a stationary server on the fixed stator winding, then the speed of the rotating magnetic field from the rotor equals the speed of the stator rotating magnetic field, namely, the synchronous speed. Both mentioned fields are locked together to give a steady torque production by the induction motor. With broken rotor bars in the motor there is an additional, backward rotating magnetic field produced, which is rotating at the slip speed with respect to the rotor. The backward rotating magnetic field speed produced by the rotor due to broken bars and with respect to the rotor is:

$$n_b = n - n_2 = n_1 \cdot (1 - s) - s \cdot n_1 = n_1 \cdot (1 - 2s) \quad \dots\dots(3)$$

The stationary stator winding now sees a rotating field at:

$$n_b = n_1 (1 - 2s) \quad \dots\dots(4)$$

or expressed in terms of frequency:

$$f_b = f_1 (1 - 2s) \quad \dots\dots(5)$$

This means that a rotating magnetic field at that frequency cuts the stator windings and induces a current at that frequency (f_b). This in fact means that f_b is a twice slip frequency component spaced $2s f_1$ down from f_1 . Thus speed and torque oscillations occur at $2s f_1$ and this induces an upper sideband at $2s f_1$ above f_1 . Classical twice slip frequency sidebands therefore occur at $\pm 2s f_1$ around the supply frequency [7, 9]:

$$f_b = (1 \pm 2s) f_1 \quad \dots\dots(6)$$

While the lower sideband is specifically due to broken bar, the upper sideband is due to consequent speed oscillation. In fact, several papers [14, 15, 16, 17, 18, 19, 21] show that broken bars actually give rise to a sequence of such sidebands given by:

$$f_b = (1 \pm 2ks) f_1 \quad k = 1, 2, 3 \quad \dots\dots k \quad \dots\dots(7)$$

Therefore the appearance in the harmonic spectrum of the sidebands frequencies given by eqn. (6) or (7) clearly indicates a rotor fault of the induction machine.

The operators of induction motor drives are under continual pressure to reduce maintenance costs and prevent unscheduled downtimes that result in lost production and financial income. Many operators now use online condition-based maintenance strategies in parallel with conventional planned maintenance schemes. This section discusses some common faults of induction motors which can be online diagnosed with help of MCSA.

A. Rotor bar analysis

The large starting currents in an induction motor, usually 5 to 8 times full load currents, occur when cooling is minimal and result in maximum thermal and mechanical stresses. The incidence of cracking in the region of the bar to end ring joint is greatest when the star-up time is relatively long and when frequent starts are required as part of a heavy duty cycle. Fractures in the rotor bars or end rings will produce amplitude and phase angle modulation of the supply current. This has

been shown to produce sidebands around the fundamental supply frequency f_1 at $(1 \pm 2S)f_1$. The relative amplitudes of these sidebands to the line frequency component form the basis for the prediction of rotor circuit health. The previous research [23] showed that an estimate of the number of broken rotor bars can be determined from the following equation:

$$R_s \approx \frac{\sin \alpha}{2p(2\pi - \alpha)} \quad \dots\dots(8)$$

where

$$\alpha = \frac{2\pi np}{R}$$

R_s = the ratio of the linear magnitude of the lower sideband at $(1-2S).f_1$ to the magnitude of the supply current f_1 .

n = number of broken rotor bars

p = pole pairs

R = number of rotor bars or slots

In practice, the sideband components are much smaller than that of the line frequency, usually 30 to 50 dB down. Thus, the calculation equation can be arranged into a decibel (dB) form so that it can be easily used with spectrum analyzers having a logarithmic scale. However, the load influence does not show up explicitly in the equation. A comparison study [24] between the predicted number of broken bars using the calculation equation and the actual number showed that the dB difference changes with load variations. It also showed that the equation underestimates the number of broken bars and hence the degree of severity of the fault, particularly at lighter loads. In order to predict broken bars with reasonable accuracy, an empirical factor has to be added in the calculations. The software package, such as ‘Motormonitor’, has taken this approach and yielded satisfactory results in the industrial environment.

$$f_{rotor} = (1 \pm 2ks) f_1 \quad \dots\dots (9)$$

The frequencies of spectral components in stator windings are given by [13, 18, 21]

Where f_1 is the electrical-supply frequency,

s is the per-unit slip, and $k = 1, 2, 3, \dots$, respectively.

B. Stator-Winding Faults

The interturn short circuit of the stator winding is the starting point of winding faults such as turn loss of phase windings. The short-circuit current flows in the interturn short-circuit windings. This initiates a negative MMF, which reduces the net MMF of the motor phase. Therefore, the waveform of airgap flux, which is changed by the distortion of the net MMF, induces harmonic frequencies in a stator-winding current as [17, 18, 21]:

$$f_{stator} = \left\{ \frac{n}{p} (1 - s) \pm k \right\} f_1 \quad \dots\dots (10)$$

Where p is the number of pole pairs, $n = 1, 2, 3, \dots$, and $k = 1, 3, 5, \dots$, respectively.

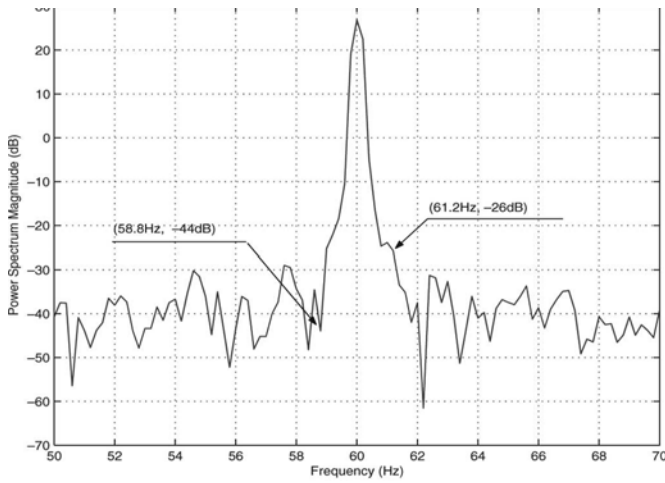


Figure 4 (a): Spectrum magnitudes of stator currents (Healthy rotor bar)

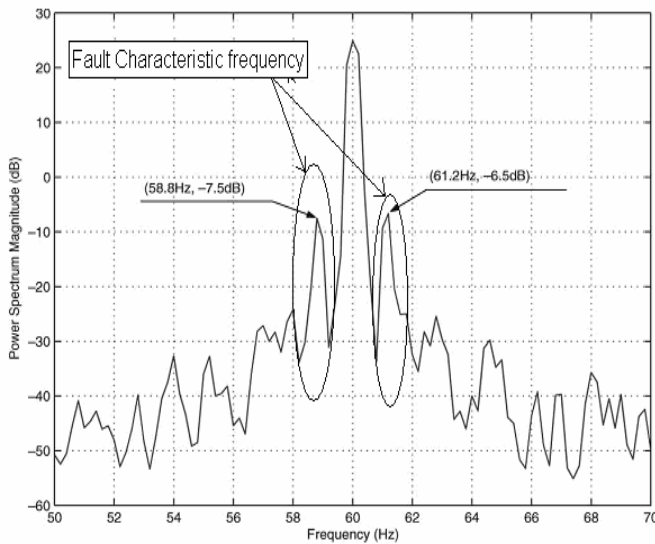


Figure 4(b): Spectrum magnitudes of stator currents (Broken rotor Bar)

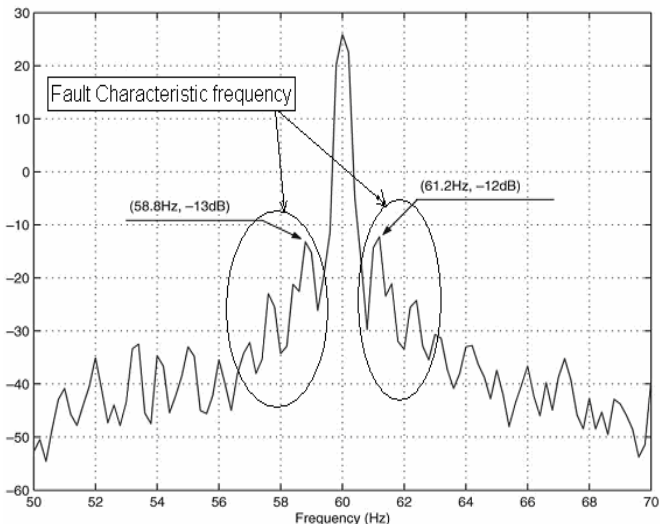


Figure 4(c): Spectrum magnitudes of stator currents (Corrosive rotor bar)

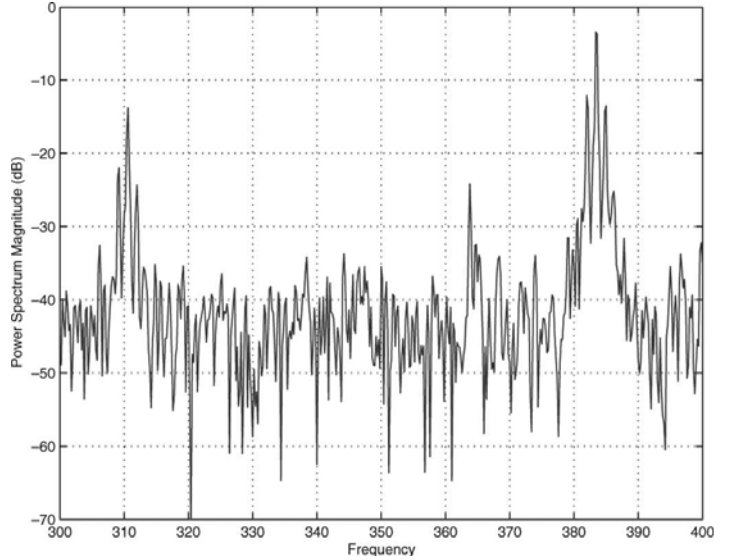


Figure 5(a): Stator-winding-fault frequency spectra (Healthy motor)

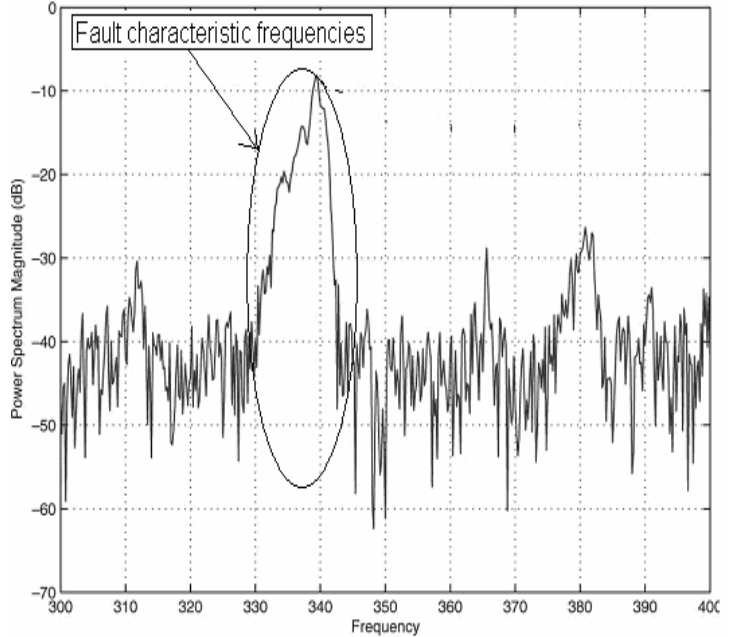


Figure 5(b): Stator-winding-fault frequency spectra (Stator-winding interturn short)

C. System under Analysis

A case-study 3-phase, 440-V, 60-Hz, 5-hp, squirrel-cage induction motor, was tested in the laboratory. This motor was tested under healthy and one through four broken bars of rotor faulty conditions while another 3- phase, 5-hp squirrel cage, induction motor was tested under inter-turn shorts faults in one phase of the stator windings.

D. Results

Fig. 4 (a), (b) and (c) show a comparison between the current spectrum for a fault free machine, corrosive and broken rotor bar. The spectral analysis clearly shows that if a rotor fault is present, some components appear at the fault's

characteristic frequencies in the spectrum. These fault characteristic frequencies are directly related to the shaft rotating frequency and its sub-harmonics. All cases have 60 Hz line frequency a 0.5-Hz slip frequency with the 2-N- m constant load. From eqn. (9), the abnormal harmonic frequencies of rotor asymmetry are obtained as 58.8 and 61.2 Hz with the harmonic constant $k = 1$ and the slip frequency 0.6 Hz. The power-spectrum magnitudes of left sidebands are shown that the healthy, corrosive, and broken rotor bar have -44 , -13 , and -7.5 dB, respectively. In addition, the power-spectrum magnitudes of the right sidebands are -26 , -12 , and -6.5 dB, respectively. Power-spectrum magnitudes of the lower and upper sideband have a tendency that the power-spectrum magnitudes of the corrosive rotor bar have a position between the healthy and broken rotor bar. Fig. 5 shows the power spectrum magnitudes of stator currents obtained by conducting an experiment on 3- phase, 5-hp squirrel cage, induction motor. From eqn. (10), the abnormal harmonic frequency of a stator-winding fault, as illustrated by Fig. 5(b), appeared at 334.6 Hz with the dominant harmonic numbers $k = 1$, $n = 20$, and a slip frequency $f_{s1} = 4.6$ Hz. Here, the inter-turn short circuit of stator winding was used to realize the condition of a stator-winding fault. In order to easily investigate abnormal harmonics, large slips were introduced by a heavy load.

III. FAULT DIAGNOSIS WITH SHORT-TERM FOURIER TRANSFORMATION

It is the time-dependent Fourier transform for a sequence, and it is computed using a sliding window. The STFT is a Fourier-related transform that is used to determine the sinusoidal frequency and the phase content of the local sections of a signal as it changes over time [5]. In this method, the spectrogram is used to estimate the frequency content of a signal. The magnitude squared of the STFT yields the spectrogram of the function, which is usually represented like color plots as shown in figure 6. Moreover, these kinds of images provide graphical information of the evolution of the power spectrum of a signal, as this signal is swept through time [6]. The spectrograms are also used in industrial environments to analyze the frequency content and variation of a non-constant frequency signal. In the case of non-constant load torque of an induction motor, the spectrogram could be used to show the changes in harmonic-current amplitudes.

A. System under analysis

A case-study 3-phase, 440-V, 6-poles, 5-hp, squirrel-cage induction motor, supplied by an AC drive operating under scalar (open-loop) constant Volts per Hertz control was tested in the laboratory. This motor has a cage with 45 bars, that is $7\frac{1}{2}$ bars per pole pitch, and it has 240 stator winding turns per phase housed in a stator with 36 slots, that is six slots per pole, and hence two slots per pole per phase. This motor was tested under healthy and one through four broken bars of rotor faulty conditions.

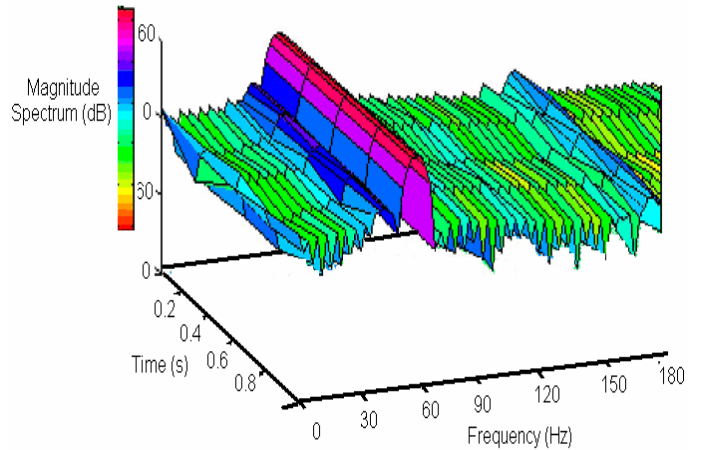


Fig. 6: Three-dimensional spectrogram details for the 0–180-Hz band, broken rotor bars.

B. Result and analysis

A short detail of the spectrogram and drawing the spectral distribution of a signal along time is shown in Fig. 6. The figure is scaled in decibels to obtain the best resolution. The spectrogram shows the harmonics nearest to the main frequency in detail, which result from broken rotor bars. Spectrograms show the fault frequencies from the perspective of time variation and could, therefore, be useful techniques to apply to signals containing time-varying frequencies. In short, spectrograms give a clear idea of the band where signal-processing efforts have to be focused on. However, spectrograms are based on STFT and require high processing power to obtain good resolution. Thus, an improved processing method is needed, and wavelet transform may be a good choice [31].

IV. FAULT DIAGNOSIS WITH WAVELET TRANSFORM

Fourier analysis uses the basic functions $\sin(t)$, $\cos(t)$, and $\exp(it)$. In the frequency domain, these functions are perfectly localized, but they are not localized in the time domain, resulting in a difficult to analyze or synthesize complex signals presenting fast local variations such as transients or abrupt changes [28]. To overcome the difficulties involved, it is possible to "window" the signal using a regular function, which is zero or nearly zero outside a time segment $[-m, m]$. The results in the windowed-Fourier transform [30]:

$$G_s(w, t) = \int s(u)g(t-u)e^{-iwu} du \quad \dots\dots(11)$$

Shifting and scaling a different window function, called in this case mother wavelet, it is obtained the so called Wavelet Transform.

$$G_s(w, t) = \int s\left(\frac{1}{\sqrt{a}}\right)\varphi\left(\frac{t-u}{a}\right) du \quad \dots\dots(12)$$

where a is the scale factor, u is the shift, $\varphi(t)$ is the mother wavelet and $G_s(w, t)$ is the wavelet transform of function $s(t)$.

The discrete version of Wavelet Transform, DWT, consists in sampling not the signal or not the transform but sampling the scaling and shifted parameters. This result in high frequency resolution at low frequencies and high time resolution at high frequencies, removing the redundant information .

A discrete signal $x[n]$ could be decomposed:

$$x[n] = \sum_k a_{j_0,k} \phi_{j_0,k}[n] + \sum_{j=j_0}^{j-1} \sum_k d_{j,k} \varphi_{j,k}[n] \dots\dots(13)$$

where

$\phi[n]$ = scaling function

$\phi_{j_0,k}[n] = 2^{j_0/2} \phi(2^{j_0}n - k)$: scaling function at scale

$s = 2^{j_0}$ shifted by k .

$\varphi(n)$: mother wavelet

$\varphi_{j_0,k}[n] = 2^{j/2} \varphi(2^j n - k)$: scaling function at scale

$s = 2^j$ shifted by k .

$a_{j_0,k}$: Coefficients of approximation at scale $s = 2^{j_0}$

$d_{j,k}$: Coefficients of detail at scale $s = 2^j$

$N = 2^j$: being N the number of sample of samples of $x[n]$

In order words, a discrete signal could be constructed by means of a sum of a $j - j_0$ details plus a one approximation

of a signal at scale $s = 2^{j_0}$

The details and the approximations at different scales could be obtained by means of a tree decomposition showed in Fig. 7.

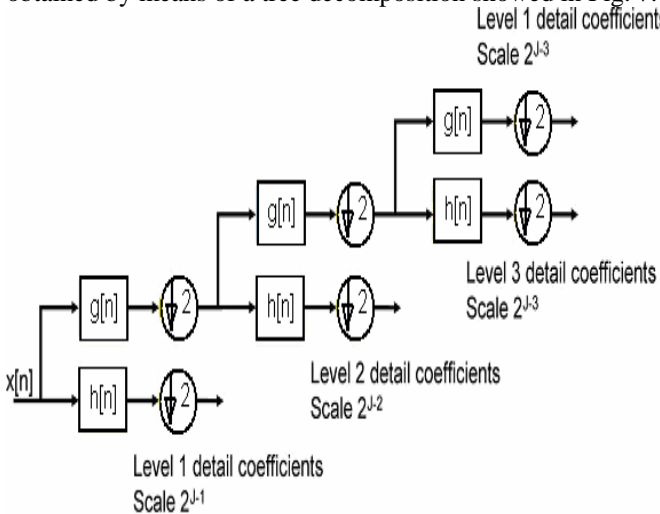


Fig. 7: Wavelet tree decomposition with three-detail levels.

A. System under analysis

In this experiment, two induction motors 1.5 kw, 440V was investigated for monitoring and diagnosis of broken rotor

bars which were artificially damaged. The fig. 9 presents the results of an experiment.

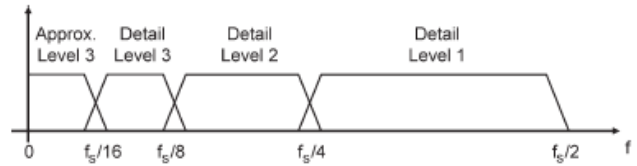


Fig. 8: Frequency ranges cover for details and final approximation.

Figure 9 (a): Wavelet decomposition for a healthy induction

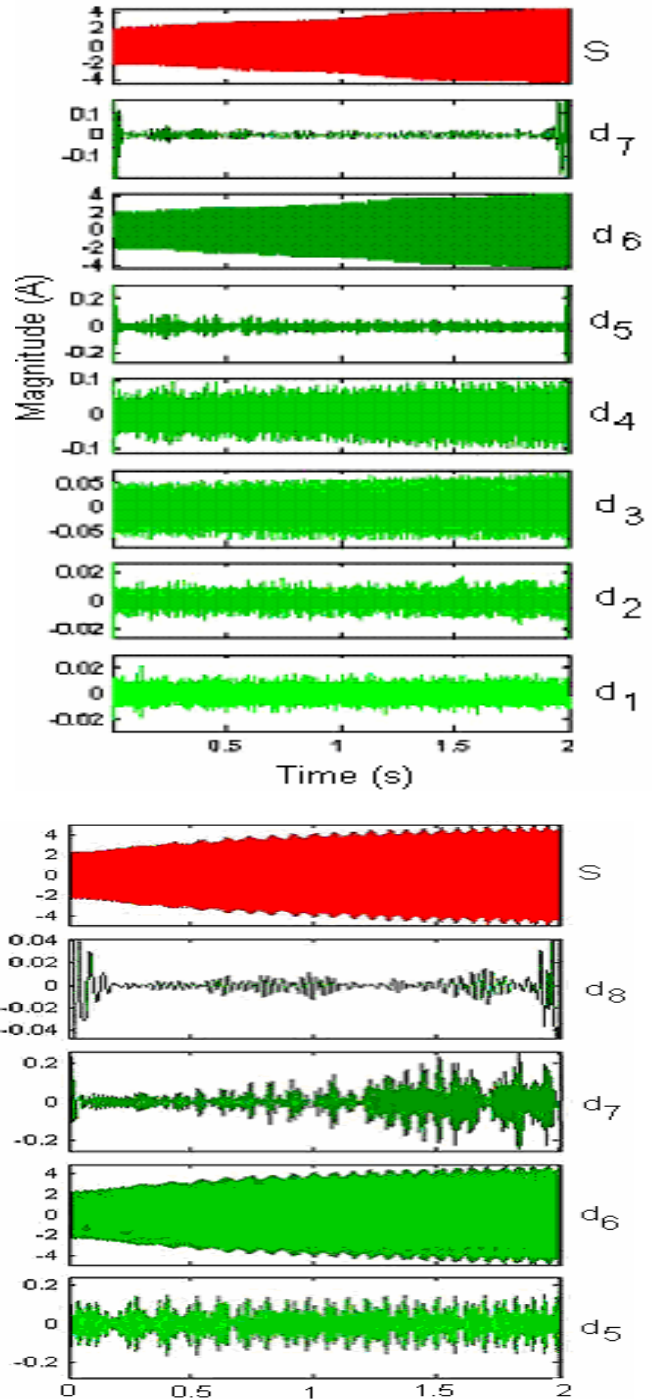


Fig 9(b): Wavelet decomposition for IM with broken bars.*B. Result and analysis*

The motors were tested both under constant and non-constant load torque. Under non-constant load torque, it was expected that the amplitude of the harmonics and their frequencies over the spectrum will change continuously. The wavelet analysis breaks up the signal in several details and one final approximation. The different components cover the entire frequency spectrum with different bandwidths. The frequency bands depend on the sampling frequency and decrease as shown in Fig. 8. The highest band, which corresponds to level-one decomposition, covers from $f_s/2$ to $f_s/4$. For the next decomposition level, both the center frequency and the bandwidth divided into two.

Figs. 9 (a) and (b) show the wavelet decomposition, from levels five to seven, for a healthy motor and for a faulty motor, respectively. For the lower decomposition levels (high frequency bands), there is no information about signal variation available, and the wavelet decomposition appears virtually only as a ground line. Low frequency details five to seven are much more relevant for fault detection, because they cover the frequency band corresponding to the supply and the fault frequency [31]. Detail seven is primarily tuned with the fault harmonic band, and it should be the preferred option in diagnosing the condition of the motor. In case of a short circuit produced between turns in a stator phase, not only an unbalance appears in the currents but also fault harmonics due to it.

V. CONCLUSION

In this paper, Motor current signature analysis for the detection of induction motor faults based on FFT, STFT, and wavelet analysis of stator current are discussed with some experimental results which are useful for online diagnosis in industrial applications. MCSA detects changes in a machine's permeance by examining the current signals and uses the current spectrum of the machine for locating characteristic fault frequencies. The spectrum is obtained using a Fast Fourier Transformation (FFT) that is performed on the signal under analysis. The fault frequencies that occur in the motor current spectra are unique for different motor faults. However this method does not always achieve good results with not constant load torque. Therefore, this paper proposes a different signal processing methods, such as short time Fourier transforms (STFT) and wavelet analyses. The STFT determines the sinusoidal frequency and the phase content of the local sections of a signal as it changes over time. In this method, spectrogram is used to estimate the frequency content of a signal. The magnitude squared of the STFT yields the spectrogram of the function, which is usually represented like color plots. On other hand, Wavelet transforms show changes on harmonics amplitude and distribution, and it is the suitable transform to be applied on non stationary signals. At last, we can conclude that the new methods such as Short-Time

Fourier Transform (STFT) and wavelet analysis can effectively diagnose shorted turns and broken rotor bars in non-constant-load-torque induction-motor applications.

REFERENCES

- [1] Neelam Mehala & Ratna Dahiya, "An Approach of Condition Monitoring of Induction Motor Using MCSA", *International Journal of System Application, Engineering and Development*, Vol. 1, no.1, 2007, pp.13-17.
- [2] Neelam Mehala, Ratna Dahiya, "Motor Current Signature Analysis and its Applications in Induction Motor Fault Diagnosis", in *proc. of 7th WSEAS International conference on Signal Processing, Robotics and Automation (ISPRA-08)*, Cambridge, UK, Feb. 20-22, 2008, pp. 442-448. C.
- [3] B. Vilakazi, T. Marwala, P. Mautla, E. Moloto, "On-line Condition Monitoring using Computational Intelligence", *WSEAS Transactions On Power Systems, Issue 1*, Volume 1, January 2006. pp. 280-286.
- [4] Niaoqing Hu, Yue Zhang, Fengshou Gu, Guojun Qin, Andrew Ball, Early, "Fault Detection using A Novel Spectrum Enhancement Method for Motor Current Signature Analysis", in *proc. of 7th WSEAS Int. Conf. on Artificial Intelligence, Knowledge Engineering And Data Bases (AIKED'08)*, University of Cambridge, UK, Feb 20-22, 2008. pp. 470-475.
- [5] Reza Haghmaram, Abbas Shoulaie, "Parameters Effects on Force in Tubular Linear Induction Motors with Blocked Rotor", *WSEAS Transactions On Power Systems*, Issue 1, Volume 1, January 2006. pp. 55-60.
- [6] Benbouzid, M.E.H., "A review of induction motors signature analysis as a medium for faults detection", *Proc. of the 24th Annual Conf. of the IEEE*, Vol. 4, 1998, pp.1950-1955.
- [7] Thomson, W.T., And Gilmore, R.J., "Motor Current Signature Analysis to Detect Faults in Induction Motor Drives – Fundamentals, Data Interpretation, and Industrial Case Histories", *Proc. of 32nd Turbo-machinery Symposium*, Texas, A&M University, USA,,2003, pp.176-182
- [8] Milimonfared, J. et al. (1999), "A Novel Approach for Broken Rotor bar Detection in Cage Induction Motors", *IEEE Tran. On Industry Applications*, 1999, vol. 35, pp. 1000-1006.
- [9] Loránd S., Barna D.J., Ágoston B.K., "Quality and Testing, Robotics", *Inter. Conf. on Automation*, Cluj-Napoca, Romania 2004, pp..200-206.
- [10] Cho, K.R., Lang, J.H., Umans, S.D., "Detection of broken rotor bars in induction motors using state and parameter estimation", *Industry Applications*, Vol. 28, 1992, pp. 702-709.
- [11] Alexander G. Parlos, Kyusung Kim & Raj Bharadwaj, "Detection of Induction Motor Faults - Combining Signal-based and Model-based Techniques", *Proc. of the American Control Conf.* Anchorage, AK, 2002, pp. 4531-4536.

- [12]Filippetti F, Franceschini G. Tassoni, C., Vas P., “Broken bar detection in induction machines: current spectrum approach and parameter estimation approach”, *Industry Applications Society*, Vol.1, 1994, pp. 95-102.
- [13]Hargis C., Gaydon B. G., & Kamash K., “The Detection of Rotor Defects in Induction Motors”, *Proc. of the Instt. of Electrical Engineers (IEE), Conf. on Electrical Machines - Design and Applications*, 213,1982, pp. 216-220.
- [14]Thomson W. T., Chalmers S. J., & Rankin D., “On-Line Current Monitoring Fault Diagnosis in HV Induction Motors - Case Histories and Cost Savings in Offshore Installations”, *Proc. of Society of Petroleum Engineers (SPE) (Offshore Europe’87, Aberdeen, Scotland)*, 1987, pp.1-19 .
- [15]Cameron J. R., Thomson W. T.& Dow A. B., “Vibration and Current Monitoring for Detecting Airgap Eccentricity in Large Induction Motors”, *Proc. of the Instt. of Electrical Engineers*,1986,pp.55-163 .
- [16]Thomson, W. T., Cameron, J. R. & Dow A. B., “On-Line Diagnostics of Large Induction Motors, *NATO Advanced Research Workshop on Vibrations and Noise in Alternating Current Machines*”,(Catholic University, Leuven, Belgium), 1986, pp.1-20 .
- [17]Kliman G. B., Koegl R. A., Stein J., Endicott R. D.& Madden M. W., “Noninvasive Detection of Broken Rotor Bars in Operating Induction Motors”, *IEEE Trans. on Energy Conversion*, Vol. 3, 1988, pp. 873-879 .
- [18]Jung J.H., Jong-Jae Lee & Bong-Hwan Kwon, “Online Diagnosis of Induction Motors Using MCSA”, *IEEE Trans. on Industrial Electronics*, Vol. 53, 2006, pp.1842-1852.
- [19]Schoen R., Habetler T.G., Kamran F. & Bartfield R.G., “Motor bearing damage detection using stator current monitoring”, *IEEE Trans. Ind. Appl.*, Vol. 31, 1995, pp.1274–1279.
- [20]Hachemi Benbouzid M.El., “A review of induction motors signature analysis as a medium for faults detection”, *IEEE Trans. Ind. Electron.*, Vol. 47, 2000, pp. 984–993.
- [21]Neelam Mehala & Ratna Dahiya, “Motor Current Signature Analysis and its Applications in Induction Motor Fault Diagnosis”, *International Journal of Systems Applications, Engineering & Development*, Vol 2,2007, pp. 29-35.
- comparison between
- [22]D. C. Robertson, O. I. Camps, and J. S. Mayer,) “Wavelets and power system transients: Feature detection and classification,” in *Proc. Int. Symp. Optical Engineering in Aerospace Sensing*, vol. 2, 1994, pp. 474–487.
- [23]S. Santoso, E. J. Powers, and W. M. Grady, “Power quality assessment via wavelet transform analysis,” *IEEE Trans. Power Delivery*, vol. 11, 1996, pp. 924–930.
- [24]P. Pillay and A. Bhattacharjee, “Application of wavelets to model shortterm power system disturbances,” *IEEE Trans. Power Syst.*, vol. 11, 1996, pp. 2031–2037.
- [25]A. W. Galli, G. T. Heydt, and P. F. Riberio, “Exploring the power of wavelet analysis,” *IEEE Computer. Application. Power*, vol. 9, 1996, pp. 37–41.
- [26]P. Pillay, P. Ribeiro, and Q. Pan, “Power quality modeling using wavelets,” in *Proc. Int. Conf. Harmonic and Quality of Power*, 1996, pp. 625–631.
- [27]A. Gaouda and M. Salama, “Wavelet-based signal processing for disturbance classification and measurement,” *Proc. IEEE—Generation, Trans., Distribution.*, vol. 149, no. 3, 2002, pp. 310–318.
- [28]P. S. Meliopoulos and C. H. Lee, “Wavelet based transient analysis,” *IEEE Transact. Power Delivery*, vol. 15, 2000, pp. 114–121.
- [29]I. Daubechies, “Orthonormal bases of compactly supported wavelets,” *Commun. Pure Appl. Math.*, vol. 41, 1988, pp. 909–996.
- [30]P. F. Ribeiro, “Wavelet transform: An advanced tool for analyzing nonstationary harmonic distortions in power systems,” in *Proc. IEEE Int. Conf. Harmonics in Power Systems*, 1994, pp. 141–149.
- [31]Jordi Cusidó, Luis Romeral, Juan A. Ortega, Javier A. Rosero, and Antonio García Espinosa , “Fault Detection in Induction Machines Using Power Spectral Density in Wavelet Decomposition, *IEEE Transactions On Industrial Electronics*, Vol. 55, No. 2, 2008, pp. 633-643.
- [32] S. G. Mallat, “A theory for multi-resolution signal decomposition: The wavelet representation,” *IEEE Trans. Pattern Anal. Machine Intelligence*, vol.7, 1989, pp. 674–693.